Corresponding Author: Dr. Sushanta Debnath, Ph.D.

Corresponding Author's Institution: University of Johannesburg

First Author: Sushanta Debnath, Ph.D.

Order of Authors: Sushanta Debnath, Ph.D.; Kriveshini Pillay, PhD; Niladri Ballav, PhD; Hlengilizwe Nyoni; Arjun Maity, PhD

The Editor in Chief   25/05/2014

Applied Catalysis B: Environmental

Elsevier

SUBMISSION OF MANUSCRIPT

Dear Editor,

Please find the manuscript titled "**Optimization and Mechanism Elucidation of the Catalytic Photo-Degradation of the Dyes Eosin Yellow (EY) and Naphthol blue black (NBB) by a Polyaniline-coated Titanium Dioxide Nanocomposite**", which I submit for consideration of publication in your esteemed journal. The In this connection, I report that this is an original work and that the manuscript is not submitted in any other journal for publication. I hereby confirm that all the authors mutually agreed to submit the article in **Applied Catalysis B: Environmental** and there is no confliction. I hope this article perfectly fits the scope and suitability for **Applied Catalysis B: Environmental**.

Your rapid decision will be highly appreciated.

With regards,

Sushanta Debnath,
Department of Applied Chemistry
University of Johannesburg
South Africa

Suggested Reviewers:

1. Uday C Ghosh, Ph.D

Emeritus Associate Professor, Department of Chemistry and Bio Chemistry, Presidency
University,

ucghosh@yahoo.co.in

Dr. Ghosh has a number of publications in internationally reputed journals in this field
and is an experienced researcher.

2. Kunal Das Ph.D

Nanjing University of Information Science and Technology

kunalchemdas@gmail.com

Dr. Das is very well known in material synthesis and has lots of publication in this field
.

3. Ahmad Fikri Ph.D

Lecturer, Department of Biological and Agricultural Engineering, Universiti Putra
Malaysia

fikri@eng.upm.edu.my

Dr. Fikri works on water Science and technology and has reputed publications in this
field.

Optimization and Mechanism Elucidation of the Catalytic Photo-Degradation of the Dyes Eosin Yellow (EY) and Naphthol blue black (NBB) by a Polyaniline-coated Titanium Dioxide Nanocomposite

Sushanta Debnath,[a,*] Niladri Ballav,[a] Hlengilizwe Nyoni,[a] Arjun Maity,[b,c] Kriveshini Pillay[a]

[a] Department of Applied Chemistry, University of Johannesburg, Johannesburg, South Africa

[b] National Centre for Nano-structured Materials, Council of Scientific and Industrial Research, Pretoria, South Africa

[c] Department of Civil and Chemical Engineering, University of South Africa (UNISA), South Africa

*Corresponding author

Tel:+27 11 5596128

Fax: +27 11 5596425

Email:

sushanta.debnath@yahoo.com (S. Debnath)

kriveshinip@uj.ac.za (K.Pillay)

ABSTRACT

A polyaniline-coated titanium oxide nanocomposite (PTO) was synthesized, characterized and used in the catalytic photo-degradation of the azo-dyes Eosin Yellow (EY) and Naphthol blue black (NBB). An emphasis was placed on the key parameters governing the degradation process. It was noted that the extent of degradation was higher at lower pH for both dyes. The rate of degradation of both dyes also increased with increasing catalyst dosage and together with Langmuir-Hinselwood models and other second-order kinetic models verified that heterogeneous photocatalysis occurred. The rate of degradation increased with increasing initial dye concentrations and only increased gradually with an increase in UV light intensity in the absence of the catalyst. The optimum operating conditions for the degradation was also predicted using Response Surface Methodology (RSM) analysis as a statistical tool. This analysis revealed that the initial dye concentration, pH and dosage of the catalyst are all significant parameters in the degradation process. The combined effect of pH and initial concentration was antagonistic whilst the combined effect of initial concentration and catalyst dosage and the combined effect of catalyst dosage and pH were both synergistic. The optimum degradation percentages were found to be 99.85 and 99.74 for EY and NBB respectively. These optimum percentage degradations were observed at pH 3.0, initial dye concentration 15 mg L^{-1} and a catalyst dosage of 1.0 g L^{-1}. LC-MS data was also used to identify the photodegradation products and to propose a mechanism of photodegradation.

Keywords: Photocatalytic degradation; Eosin Yellow, Naphthol Blue Black; Polyaniline coated titanium oxide nanocomposite; Response Surface Methodology

Introduction

Textile dyes and other dyestuffs which are used in industrial applications like paper and pulp, adhesives, art supplies, beverages, ceramics, cosmetics, food, paints etc constitute a class of compounds which increases the environmental pollution load to a large extent. Among the dyes, the azo-class of dyes with aromatic moieties linked with azo bond ($-N = N -$) acquires the majority of the share (50-70 %) of the dyes used in textile and other industries [1,2]. About 1-20 % of the used dye remains unfixed and the same is discharged in the waste effluent causing the coloration of the wastewater and threat to the aquatic life [3,4]. The dyes itself and its degradation products are highly carcinogenic and mutagenic [5-9]. Thus, removal of the dye and their degraded products is highly essential in view of the environmental hazard that this poses as well as the threat to human health.

Reactive dyes are highly soluble in water and their removal from aqueous solution by conventional coagulation and filtration, activated sludge processes, adsorption, biological treatment, chlorination, ozonation, flocculation, reverse osmosis are insufficient for the wastewater treatment either for not being cost-effective or not being destructive enough [10-16]. The non-destructive processes only transfer the pollutant from one phase to other, which further requires treatment and a different kind of pollution is faced. The advance oxidation process (AOP) is one of the treatment methods which have been extensively studied [17-19]. AOPs are based on the generation of hydroxyl radicals ($OH^{\bullet}$) which are very active in degrading different classes of organic pollutants [20,21].

With comparison to the AOPs, heterogeneous photocatalysis is considered as a cost effective and environment friendly alternative for the refinement of the dye containing wastewater [22,23]. The use of TiO_2 (TO) and its composites under UV irradiation has been extensively studied for degrading and mineralizing of reactive dyes from dye containing solutions [11,24-28]. TiO_2 based materials are good photocatalysts due to low band gap energy of TiO_2 compared to other photocatalysts. Some TiO_2 based photo catalysts reported by other authors are $SrTiO_3$ composite [29], CdS embedded TiO_2 nano-spheres [30], $AgAlO_2/TiO_2$ composite [31], TiO_2/Ag composite [32], Cu doped TiO_2 thin film [33] etc. Photocatalysis does not require any oxidizing chemicals and can be operated at mild conditions of temperature and pressure.

The limitation of the photocatalysts lies in the existence of the partially degraded intermediates into the reaction solution which could not be removed by photo catalysis, or can be removed by prolonged UV irradiation only. This decrease the cost effectiveness of the process. To overcome this drawback, the photocatalyst could be coated with some compounds which are able to remove the intermediates by adsorption and as a result contaminant free final aqueous solution could be regained.

Most of the studies conducted to date do not report the interaction of all the independent variables used in the degradation studies. Response surface methodology (RSM) is the statistical tool which correlates the inter-dependent relation between the degradation process variables [34]. Based on some experimental data, RSM can optimize the degradation process. To date, no correspondences are known to establish the optimization of degradation of Eosin Y (EY) and Naphthol blue black (NBB) by polyaniline coated TiO_2 (PTO) applying the RSM.

In this communication, we have used a PTO nanocomposite for the degradation of two dyes, EY and NBB from their aqueous solution. The parameters varied are the pH, catalyst dose, initial dye concentration and UV light intensity. The degradation percentage of the dye was monitored by the change in COD content of the effluent at different course of reaction. The results are analyzed using degradation kinetic parameters e.g Langmuir- Hinshelwood equation and second order equation. Three factor central composite design (CCD) combined with RSM is applied to optimize the response as the degradation percentage of EY and NBB using PTO (photocatalyst dosage, pH and the initial dye concentration is varied during the degradation). Finally, the degraded products were identified by LCMS study and a mechanism of degradation was proposed based on the LCMS results.

2. Materials and methods

2.1 Reagents

EY (M.W. 647.89, $C_{20}H_8Br_4O_5$) and NBB (M.W. 616.49, $C_{22}H_{14}N_6Na_2O_9S_2$) used in the preparation of synthetic dye stock solution were purchased from Sigma Aldrich. The molecular structure of EY and NBB are given in **Figure S1 (Supplementary materials).** The working solutions with known dye concentrations were thereafter prepared by diluting the stock solution using distilled water. Titanium (IV) oxide (TO) nanoparticles (21 nm) (Aeroxide^{TM}) (purity:

99.5%) and ammonium persulfate as an oxidant for aniline polymerization were also purchased from Sigma Aldrich. All other reagents used were of analytical grade.

2.2 Preparation of polyaniline coated titanium oxide (PTO) nanocomposite

Polyaniline (PANI) coated titanium oxide (PTO) composite was synthesized by in situ polymerization of aniline (ANI) monomer in presence of titanium dioxide (TO) nanoparticles. 5.0 g of TO was suspended in 500 mL 0.1 N HCl solution and stirred on a magnetic stirrer for 1 h. Thereafter, 1mL of ANI was injected into the TO suspension and stirred for another 1 h to solublize the ANI molecules. Finally, 10 mL of 1 % (v/v) aqueous solution of ammonium persulfate (APS) was added to the suspension and stirred for overnight. The PANI coated TO particles were separated from the polymerization solution by means of filtration using 0.45 μm membrane filter and washed with acetone to remove the oligomers and unreacted monomers. The greenish mass was finally washed with double distilled water and dried at 60 $^{\circ}$C under vacuum.

2.3 Instruments

The following instruments were used in the experimental work: (i) Thermo pH meter (model: Orion 4 star) for pH analysis, (ii) Rigaku X-ray diffractometer for the X-ray diffraction (XRD) analysis, (iii) Föurier Transform Infra Red (FTIR) spectrophotometer (Perkin Elmer (U.S.) Spectrum 100) for FTIR spectra, (iv) Micromeritics ASAP 2020 BET surface analyzer for surface area and pore size measurement (v) UV - visible spectrophotometer (Shimadzu 1800) for colorimetric analysis of the dyes and the diffuse reflectance spectrophotometry (vi) UV lamps (25W and 15W) for irradiation in the reactor was purchased from Philips and (vii) Waters 3100 HPLC/MS was used for LCMS of the degraded products

2.4 Experimental setup of the photo-reactor for degradation

The photodegradation of the EY and NBB dye was performed in an annular reactor as shown in the schematic diagram as **Figure 1**. The dye solution was passed through the annular reactor using a peristaltic pump at different flow rates. The dye solution was stirred in a beaker using a magnetic stirrer to prevent the catalyst particles from settling down and to equilibrate the dye solution with the catalyst particles before entering the reactor. At a fixed time interval, 2 mL solution was collected from the sampling port and the residual dye concentration was measured

using UV-visible spectrophotometer after filtering through 0.45µM syringe filter. The parameters varied in the whole process are photocatalyst (PTO) dosage, pH and initial dye concentration in the reactor.

2.5 Kinetic equations of degradation of EY and NBB by PTO

The kinetics of degradation was observed by subjecting the experimental points with kinetic models viz., second order and Langmuir Hinshelwood models.

The second order equation is given as [35],

$$C = \frac{C_o}{1+k_2 C_o t}$$ --- (1)

where, k_2 (mg.g^{-1}.min^{-1}) is the second order rate constant and C_o and C (mg.L^{-1}) are the dye concentration at initial and at time 't'.

The Langmuir - Hinshelwood equation of heterogeneous catalysis is given as [36],

$$\ln\left(\frac{C}{C_o}\right) = -k_T k_a t = -k_{LH} t$$ -------------------------- (2)

$$k_{LH} = k_T k_a$$ --(3)

The half life of the reaction is calculated from the equation,

$$t_{1/2} = \frac{0.693}{k_{LH}}$$ --- (4)

where, k_T, k_a and k_{LH} (min^{-1}) are the specific reaction rate constant for the oxidation of the reactant, equilibrium constant of the reaction and the Langmuir - Hinshelwood model rate constant, respectively. Co and C are the same as equation 1.

2.6 Response surface methodology (RSM) and data analysis

The RSM is a statistical analysis method which uses the quantitative data available from some experimental design and develops the regression model equations, which are useful in predicting and optimizing the operating conditions of some processes [34,37-39]. The mutual dependency of the variables which influence the system could be understood in this method. In this paper RSM is utilized to understand the interdependent relations between the operating variables in the

degradation system, namely, initial concentrations of the dyes (EY and NBB), pH of the degradation system and mass of the photocatalyst (PTO).

This study was performed by employing the widely used standard RSM design – central composite experimental design (CCD). The chief advantage of using CCD study is to minimizing the total number of experimental runs for determining the response effect. The CCD of this study is related to 3 numerical factors (centre points) and one α value of 1.682. The CCD is considered of three independent variables: mass of the photocatalyst (m, g), concentration of the influent dye solution in the reactor (C, mg.L^{-1}) and pH of the system. The observed response is the degradation efficiency of the dyes after 150 minutes (D, %). Three levels were assigned for all the independent variables and the coded variables (C, pH and m,) with the actual values and the response (D) are shown in **Table 1**. Total 20 runs were designed to run the system and a quadratic model was employed to investigate the interaction between the independent and the dependent variables [34].

$$Y = \beta_o + \sum \beta_i X_i + \sum \beta_{ii} X_i^2 + \sum \beta_{ij} X_i X_j$$

where, Y is the predicted response, β_o is the constant of the quadratic equation, β_i is the linear coefficient, β_{ii} is the squared coefficient and the β_{ij} is the cross product coefficient.

Analysis of the experimental data according to the RSM was performed using DESIGN EXPERT 7 software. The software was also employed to statistically evaluate the surfaces created according to the following criteria: (i) each variable must present a 'p' – value (the value of probability) less than 0.05 (< 0.05) which implies that the term is significant at 95 % confidence limit, (ii) the value of regression (R^2) should be closer to unity, which means that the predicted data are close to the real data points, (iii) the "lack of fit" must be significant ('p' $<$ 0.05), which means that the model is adequate to describe the experimental data and eventually (iv) the residuals generated between the fitted data points and the experimental data points must present a normal distribution to validate the assumptions made by the *ANOVA* analysis [34].

3. Results and discussion

3.1 Characterization of the photo catalyst

3.1.1 Surface area and pore size

The BET surface area and the pore size distribution profile were determined by N_2 adsorption/desorption isotherm technique (**Fig. S2: Supplementary materials**). The degassing was done at 120 ^{o}C for 5 h and the analysis was done at -197.4 $^{\circ}$C in a liquid nitrogen bath at an equilibration rate of 10s. The BET surface area of PTO was found to be 49.81 $m^2.g^{-1}$. The surface area of the TO particles was reported to be 65 $m^2.g^{-1}$ by the manufacturer [40]. Decrease in surface area after coating indicates increase in the size of the particles, which supports successful coating of TO by PANI. The average pore width of the composites was found to be 311.19 Å.

3.1.2 Diffuse reflectance spectroscopy

The diffuse reflectance spectrophotometry of TO and PTO were performed by using $BaSO_4$ as blank in an ISR-240A Integrating Sphere Attachment attached in to the UV-Visible spectrophotometer. The band gap energies of TiO_2 and PTO were calculated by plotting the values of $[F(R)*h\upsilon]^n$ against the photon energy ($h\upsilon$). The value of 'n' depends on the type of the electronic transition which is 1 for direct and ½ for indirect band gap of a semiconductor of crystalline nature [41].

The extrapolation of the tangent of the plot on x axis gives the band gap energy of the semi conductor. **Figure 2** shows the plot of $(K*h\upsilon)^{1/2}$ versus hυ to calculate the band gap energy of TiO_2 and PTO. The band gap energies for TiO_2 and PTO are found to be 3.2 eV and 2.59 eV, respectively, which indicated PTO to be a better photocatalyst than the pure unmodified TiO_2.

3.1.2 SEM and TEM image of PTO

The SEM image of PTO and TO with the EDS spectra are given in **Figure 3A** and **B**, respectively. The SEM image of PTO indicates bigger particle size than the TO, which in turn confirms the coating of the TO particles with PANI, hence increasing in the size. The EDS analysis with weight percentage of constituent elements indicates presence of C, N, O and Ti which is the indication of successful compositing of the TiO_2 particles with PANI, whereas, the EDS of the TO only contains Ti and O. The globular coated particles are also visible in the SEM image.

As shown in **Figure 3B,** TEM images of the PTO composites are of irregular shape with PANI backbone embedded with TO nanoparticles. This suggests the successful coating of TO by PANI. The average TO nanoparticles sizes are in the range of 15-25 nm with inter lattice distance of 0.34 nm (**Figure 3B)**

3.1.3 FTIR spectra of PTO

Figure 4 shows the FTIR spectra of PTO before and after EY and NBB degradation study. Peaks at 1565, 1487, 1306 and 1143 cm^{-1} are the peaks of quinonoid ring vibration, benzenoid ring vibration, C−N stretching and $-NH^+ =$ stretching vibration of PANI, respectively [42]. The general nature of the PTO before and after degradation and adsorption remained unchanged, which implies that after degradation and adsorption, the structure of PTO is unaltered, which in turn confirms about stable coating of TiO$_2$ by PANI.

3.1.4 XRD image of PANI-TiO$_2$

The X-ray diffraction (XRD) spectra of PTO was recorded at room temperature using a powder diffractometer (Rigaku) employing the CuK$_\alpha$ radiation (λ = 0.154 nm). The scans were performed at a 2θ = 10 to 80 ^{o} at a scan rate of 1 degree per minute and shown in **Figure S3:(supplementary materials)**. The prevalent peaks are at 25.3^o, 27.7^o, 36.1^o, 37.7^o, 41.2^o, 48.0^o, 54.3^o, 62.8^o, 69.06^o and 75.1^o which are all signature peaks of anatase phase of TiO$_2$ [43]. The strongest peak at 2θ = 25.3^o is due to 101 plane of anatase TiO$_2$ which is merged with the peak of PANI at 2θ = 25.30^o.

3.1.5 Point of zero charge (pH$_{zpc}$) of the catalyst

Point of zero charge of the material was determined by zeta potential measurement and the pH vs zeta potential along with the change of phase plot is given in **Figure S4: (supplementary materials)**. The point of zero charge (pH$_{zpc}$) of the composite was found to be 7.71.

3.1.6 UV-visible spectroscopy study of degradation of EY and NBB

Figure S5: (supplementary materials) shows the UV-visible spectra of (A) EY and (B) NBB degradation with time. The spectra shows that the large peak at λ_{max} = 520 and 620 nm for EY

and NBB, respectively, decreased gradually with the course of reaction time. The peaks below 300 nm, which are due to organic moieties present in the reaction solution also decreased with time, which indicates removal of organic compounds from the reaction solution.

3.2 Effect of pH of the solution

Degradations of EY and NBB by PTO nano-composite were investigated at pH 3.0, 6.2 and 11.0 (**Figure 5**). The pH of the solution of the dye has a great influence on degradation study [44]. The degradation of the dyes are higher in acidic solution (pH 3.0) as well as in neutral solution (pH 6.2) than in basic solution (pH 11.0). Both EY and NBB are anionic dyes due to presence of carboxylate and sulfonate groups, respectively. The dyes are adsorbed more by the positively charged PTO surface at pH 3.0 and 6.2 and hence the degradation efficiency is also higher at these two pHs (**Table 2**). Degradation is increased due to the fact that the hydroxyl radical ($^\bullet$OH) density is presumably more at the catalyst surface where it forms, which decreases into the bulk of the solution. On the other hand, the catalyst surface also exerts a negatively charged surface at the solution pH > pH_{zpc}. Hence, coulombic repulsion between the dye anions and the negatively charged catalyst surface decreases the adsorption of the dyes onto the catalyst surface. Moreover, presence of large excess of OH^- ions at high pH hinders the formation of hydroxyl radical formation [45].

3.3 Effect of photocatalyst dosage

Effects of catalyst dosage on degradation of EY and NBB were observed by adding 0.25, 0.5 and 1.0 g of the PTO catalyst in the reactor to 1 L EY and NBB solution at pH 6.2 with initial concentration of 30.0 mg.L^{-1}. **Figure 6** shows that with increase in catalyst dosage the degradation rate increases, which is a characteristic of heterogeneous photocatalysis [46]. With increase in catalyst dosage, the available active sites on the catalyst responsible for the generation of hydroxyl radical ($^\bullet$OH) increases and as a result the rate of degradation is also increased. This observation is supported by the rate constants calculated using Langmuir-Hinshelwood and second order kinetic models (**Table 2**). Both the rate constants (k_2 and k_{LH}) increase with increasing catalyst dosage, which implies the rate of degradation as well as adsorption (prevalent from increase in k_2), is also faster with high adsorbent dosage. The half life

of the intermediates decreases with increasing catalyst dosage which implies that the intermediates are degraded very fast to the mineralization of the dye molecules [47].

3.4 Effect of influent dye concentration

The effect of initial dye concentration on degradation by PTO nanocomposite is shown in **Figure 7.** Here, 0.5 g of the catalyst in 1 L of dye solutions of different initial concentration (15, 30 and 60 mg.L^{-1}) was passed into the reactor at a flowrate of 10 mL.min^{-1} under the 25W UV lamp irradiation. As the initial concentration of the dye increase, the number of dye molecule also increase at a fixed number of active photo-catalyst sites. Thus the rate of the degradation decreases. The results are shown in **Table 2**. An increase in two fold of concentration decreases the rate constant and the half life of the intermediaries' more than two folds.

3.5 Effect of UV light intensity

To investigate the effect of UV light intensity on degradation of EY and NBB by the catalyst, two UV lamps of power 15W and 25W were employed with initial EY and NBB concentration of 30 mg.L^{-1}. The experiments were conducted in presence of light only without adsorbent and with presence of adsorbent in absence of light (**Figure 8**). The results show that, with increase in UV light intensity from 15 W to 25 W, in case of EY, the rate of degradation increases from 0.016 to 0.027 min^{-1} and from 0.012 to 0.023 min^{-1}, in case of NBB. The increase in degradation rate is due to increase in generation of more number of $^{\bullet}$OH on the catalyst surface in presence of higher intense light. In the absence of a catalyst and the presence of UV light, the degradation rate is abnormally low with very high half-life. This indicates that there may be some bond breaking of the dye molecules in the presence of UV light with no effective decrease in dye concentration. In the presence of catalyst in the system without UV light (in dark), the decrease in color is due to adsorption only (R^2 for second order model = 0.9207 and 0.9124) (**Table 2**), which indicates that adsorption on the catalyst surface is the major phenomena in this case rather than degradation.

3.6 Analysis of variance (ANOVA) and statistical analysis

Table 3 shows the results of results of the RSM fitting of the experimental data set in the form of analysis of variance (*ANOVA*). The *'F' value* and the *Prob.>F value* are the main indicators

which determines the significance and the adequacy of the model [34]. The *Prob.> F* less than 0.05 indicate the model to be suitable one and greater than 0.1 is considered to be of less importance [48]. The *ANOVA* of this model for both the dyes used for degradation study (EY and NBB) demonstrated that the parameters are highly significant, which is evident from the low *'F' value* (32.00 and 15.84 for EY and NBB, respectively) and very low *Prob. > F* (< 0.001) for the model. The very low *P* value indicates that the model can be considered to be significant and adequate to express the experimental data. The response of initial concentration (C_o), pH of the solution (*pH*), photocatalyst dosage (*m*), C_o*m, $pH*m$, pH^2 and m^2 for EY degradation are all found to be significant, which is evident from their Prob.> F value less than 0.05 (**Table 3**). In case of NBB the significant terms are C_o, *pH*, *m*, C_o*pH, $pH*m$, *and* m^2.

The relationship of the approximated function of the response of degradation with the varibale parameters is developed and expressed in terms of coded factors and actual factors and are given as equation (1) and (2), for EY and equation (3) and (4), for NBB, respectively, where Y is the degradation percentage after 150 minutes of UV irradiataion in the reactor.

$$\text{EY Degradation \% (Y) (Coded factor)} = 98.62 - 2.81X_1 - 11.20X_2 + 9.43X_3 - 1.51X_1X_2$$
$$+ 2.21X_1X_3 + 5.93X_2X_3 + 0.39X_1{}^2 - 4.16X_2{}^2 - 11.87X_3{}^2 \text{ ----------(1)}$$

$$\text{EY Degradation \% (Y) (Actual factor)} = 81.57 - 0.23X_1 - 0.99X_2 + 93.12X_3 - 0.017X_1X_2 +$$
$$0.26X_1X_3 + 3.95X_2X_3 + 7.69 \times 10^{-4}X_1{}^2 - 0.26X_2{}^2 - 84.38X_3{}^2 \text{ -----(2)}$$

$$\text{NBB Degradation \% (Y) (Coded factor)} = 94.78 - 4.93X_1 - 12.69X_2 + 10.21X_3 - 3.43X_1X_2$$
$$+ 1.93X_1X_3 + 6.03X_2X_3 - 0.087X_1{}^2 - 3.14X_2{}^2 - 9.80X_3{}^2 \text{ ----------(3)}$$

$$\text{NBB Degradation \% (Y) (Actual factor)} = 84.04 - 0.08X_1 - 1.51X_2 + 77.65X_3 - 0.038X_1X_2 +$$
$$0.22X_1X_3 + 4.02X_2X_3 - 1.73 \times 10^{-4}X_1{}^2 - 0.19X_2{}^2 - 69.69X_3{}^2 \text{ -----(4)}$$

The signs and the magnitudes of the regression coefficients are the representative of the each variable on the response. A positive sign indicates that the individual variable or the interacted variables has synergistic effect on the response, wheras, the negataive sign indicates the antagonistic effect on the response [49]. As observed from **Table 4,** the concentration and pH

has antagonistic effect but catalyst dosage has synergistic effect on the degradation. The term with the highest regression coefficient is the pH, which indicates that in the overall response, pH is the dominant factor. Specifically, for both the dyes the pH value below the centre point of the experimental design correspond to the highest degree of degradation. Similarly, m has also high synergistic regression coefficient for both the dyes. This indicates that the m above the centre point of the experimental design has highest degree of degradation efficiency. This results are consistent with the **Figures 6A and 6B**.

3.7 Optimization of degradation of EY and NBB by PTO under UV irradiation using RSM

The three dimensional response surface plots were analyzed to observe the better insight of the degradation of the dyes by PTO. In each plot two variables are varied while the other varibale was kept constant. The response surface plots for EY and NBB degradation are shown in **Figures 9** to **11**. In degradation study the pH and the catalyst dosage are the most influential variables.

Figure 9 shows the simultaneous effect of pH and the adsorbent dosage on degradation of **(A)** EY and **(B)** NBB. With decrease in pH and increase in adsorbent dosage, the degradation percentage increases. This is likely the result of more active surface sites at higher catalyst dosage and increased surface positive charge at lower pH (both the dyes are anionic). This synergestic effect of the cross interaction term ($pH*m$) justifies the observation of the positive regression coefficient of the RSM analysis (**Table 4**).

Figure 10 demonstrates the simultaneous effect of initial dye concentration and pH on degradation. With increase in initial concentration the number of dye molecule per unit surface of the catalyst increases and this results in lower percentage of degradation. The increased pH value also does not favours the generation of the hydroxyl radical ($^{\bullet}OH$). This effects confirms the anatagonistic effect of the cross interaction term of of C_o and pH (C_o*pH) in the regression analysis.

Figure 11 demonstrates the interaction of initial dye concentration with the catalyst dosage. The C_o individually has the antagonistic effect on the degradation. But the cross interaction term of C_o and adsorbent dosage (m) (C_o*m) has synergistic effect on degradation (**Table 4**). The magnitude of m is relatively higher than the magnitude of the C_o. Thus the antagonistic effect of the C_o is suppressed by the synergistic effect of m and as a result the overall effect of the cross interaction between C_o and m ($Co*m$) becomes synergistic. Physically, this can attributed to the

fact that with increased catalyst dosage the active surface sites are so increased with respect to the increased dye molecules at increased C_o, the effect on degradation becomes positive.

By using the response surface design and optimization, for EY the optimum degradation percentage (99.85) was obtained at pH 3.0, initial dye concentration 15 mg.L^{-1} and catalyst dosage 1.0 g.L^{-1}. For NBB, the optimum degradation percentage (99.74) was also obtained at pH 3.0, initial dye concentration 15 mg.L^{-1} and catalyst dosage 1.0 g.L^{-1}.

3.8 Determination of the degraded products by LCMS study and proposed mechanism of the degradation

The degraded products and the intermediaries formed during the course of the degradation study were identified by the LC-MS analysis and their mass spectra were interpreted from their molecule ion peaks with respect to the m/z ('m'; the molecular weight of the intermediaries in the mass spectra). The mass spectra of the solution of EY and NBB before degradation are given in **Figure A and B**, respectively. The molecular peak of un-ionized EY (m/z = 646.7) is the main peak in **Figure A**, indicating presence of un-degraded and prevalently un-ionized form of EY in the initial solution. The other peaks present in the spectra are the representative of the ionized or the adduct product of the mother molecule.

The molecular peak of un-ionized form (m/z = 616.0) is not the major peak in the initial NBB solution. The NBB remains mainly in ionized form in the initial NBB solution, which is evident from the presence of two peaks (m/z = 571.1 and 285.1).

Figure C and D shows the degradation products of EY and NBB after 180 minutes of UV irradiation. The molecular peaks of the non degraded dye molecule are not observed at all. Although, the molecular peak of un-ionized peaks of NBB was not visible in the LCMS of the dye before irradiation, the peaks of the ionized form of the non degraded forms were also invisible in the LCMS of the product after 180 minutes of irradiation. This means that the NBB molecule also undergoes degradation under UV irradiation.

The spectrum of EY and NBB in **Figure A and B**, respectively, are different from the spectra of the irradiated EY and NBB in **Figure C and D**, respectively. The difference can be explained due to the decomposition of the dyes in different m/z in the presence of PTO.

The peaks in the spectrum of non irradiated EY (**Figure A**) at m/z ratio 646.6 and 487.2 are not observed in the spectrum of the irradiated EY (**Figure C**). Similarly, the peaks in the spectrum of non irradiated NBB (**Figure B**) at m/z ratio 285.1, 571.1 and 616.0 are not visible in the spectrum of the irradiated NBB (**Figure D**). The disappearance of these peaks therefore confirms that degradation occurred under UV radiation.

The degradation of both the dyes can be initiated by the available $OH^{\bullet}$ generated from the catalyst (PTO). The degradation of the dyes may occur through the following steps, (i) the cleavage of the aryl ring (specifically, the benzene rings at the sides of the molecules decomposes, (ii) the ionization of the dye molecules in aqueous solution (iii) cleavage of the C-S bond in NBB (iv) cleavage of various $C - O$, $C - N$ and $C - C$ bond by the attack of the $OH^{\bullet}$ and (iv) $-N = N-$ double bond cleavage.

According to the results obtained from the LCMS data, the following schemes are proposed for the degradation of EY and NBB in presence of PTO under UV light.

Conclusion

A polyaniline –coated titanium dioxide nanocomposite (PTO) has been successfully synthesized, characterized and used as a catalyst in the photo-degradation of the dyes EY and NBB. The degree of degradation increases at lower pH; increasing catalyst dosage and increasing initial dye concentrations. The effect of UV light intensity in the absence of the catalyst is not significant. Langmuir-Hinselwood and second order kinetic models have provided evidence for a heterogeneous photo-catalysis. The response-surface statistical analysis revealed that the combined effect of pH and initial dye concentration is antagonistic. Contrarily, the combined effects of catalyst dosage and pH and the combined effect of catalyst dosage and initial dye concentration are synergistic. This suggests that catalyst dosage is the most significant process parameter governing the degradation process. The optimum degradation percentages have been evaluated as 99.85 and 99.74 for EY and NBB respectively. This has been achieved at pH 3.0, initial dye concentration of 15 mg L^{-1} and a catalyst dosage of 1.0 g L^{-1}. These preliminary results therefore suggest that PTO is an efficient catalyst for the degradation of EY and NBB provided that the optimum conditions of pH, initial dye concentration and catalyst dosage are maintained. A LC-MS analysis confirmed that degradation occurred after UV irradiation and the photodegradation products were identified and provide experimental evidence for the generation

of a hydroxyl radical and decomposition of benzene ring followed by ionization of the dye molecules and cleavage of C-S, C-C,--N=N- and C-N bonds by the hydroxyl radical.

Acknowledgement

Reference List

[1] R. Molinari, F. Pirillo, M. Falco, V. Loddo, L. Palmisano, Chem. Eng. Process.: Process Intens. 43 (2004) 1103-1114.

[2] S. Bilgi, C. Demir, Dyes Pigments 66 (2005) 69-76.

[3] I.K. Konstantinou, T.A. Albanis, Appl. Catal. B-Environ. 49 (2004) 1-14.

[4] S. Song, L. Xu, Z. He, H. Ying, J. Chen, X. Xiao, B. Yan, J. Hazard. Mater. 152 (2008) 1301-1308.

[5] R.O.A. Lima, A.P. Bazo, D.M.F. Salvadori, C.M. Rech, D.P. Oliveira, G.A. Umbuzeiro, Mutat Res./Genet. Tox. En. 626 (2007) 53-60.

[6] P.A. Carneiro, G.A. Umbuzeiro, D.P. Oliveira, M.V. Zanoni, J. Hazard. Mater. 174 (2010) 694-699.

[7] F.M.D. Chequer, T.M. Lizier, R. de Felicio, M.V.B. Zanoni, H.M. Debonsi, N.P. Lopes, R. Marcos, D.P. Oliveira, Toxicol. Vitro 25 (2011) 2054-2063.

[8] D.P. Oliveira, P.C.A. Carneiro, M.K. Sakagami, M.V. Zanoni, G.A. Umbuzeiro Mutat Res./Genet. Tox. En. 626 (2007) 135-142.

[9] S. Venitt, C.C. Sleigh, M.R. Osborne, Mutat Res./Genet. Tox. 135 (1984) 31-47.

[10] C. Tang, V. Chen, Water Res. 38 (2004) 2775-2781.

[11] A. Akyol, H.C. Yatmaz, M. Bayramoglu, Appl. Catal. B- Environ. 54 (2004) 19-24.

[12] C.A.K. Gouvea, F. Wypych, S.G. Moraes, N. Duran, N. Nagata, P.P. Zamora, Chemosphere 40 (2000) 433-440.

[13] M.A. Adebayo, L.D.T. Prola, E.C. Lima, M.J.P. Rosero, R. Catalua, C. Saucier, C.S. Umpierres, J.C.P. Vaghetti, L.G. da Silva, R. Ruggiero, J. Hazard. Mater. 268 (2014) 43-50.

[14] A. Afkhami, R. Moosavi, J. Hazard. Mater. 174 (2010) 398-403.

[15] Z. Aksu, G. Donmez, Chemosphere 50 (2003) 1075-1083.

[16] S. Bai, X. Shen, X. Zhong, Y. Liu, G. Zhu, X. Xu, K. Chen, Carbon 50 (2012) 2337-2346.

[17] C. Guillard, H. Lachheb, A. Houas, M. Ksibi, E. Elaloui, J.M. Herrmann, J. Photochem. Photobiol. A: Chem. 158 (2003) 27-36.

[18] C. Hachem, F. Bocquillon, O. Zahraa, M. Bouchy, Dye Pigments 49 (2001) 117-125.

[19] V. Augugliaro, C. Baiocchi, A. Bianco Prevot, E.G. Lopez, V. Loddo, S. Malato, G. Marci, L. Palmisano, M. Pazzi, E. Pramauro, Chemosphere 49 (2002) 1223-1230.

[20] C.C. Chan, C.C. Chang, W.C. Hsu, S.K. Wang, J. Lin, Chem. Eng. J. 152 (2009) 492-497.

[21] C.H. Chiou, C.Y. Wu, R.S. Juang, Chem. Eng. J. 139 (2008) 322-329.

[22] J. Kiwi, C. Pulgarin, P. Peringer, M. Gratzel, Appl. Catal. B: Environ. 3 (1993) 85-99.

[23] S. Tanaka, T. Ichikawa, Water Sci. Technol. 28 (1994) 103-110.

[24] A.K. Gupta, A. Pal, C. Sahoo, Dyes Pigments 69 (2006) 224-232.

[25] T.S. Natarajan, M. Thomas, K. Natarajan, H.C. Bajaj, R.J. Tayade, Chem. Eng. J. 169 (2011) 126-134.

[26] M. Anpo, S. Dohshi, M. kitano, Y. Hu, M. Takeuchi, M. Matsuoka, Annual Rev. Mater. Res. 35 (2005) 1-27.

[27] M. Kanna, W. Sumpun, Mater. Chem. Phys. 110 (2008) 166-175.

[28] I.K. Konstantinou, T.A. Albanis, Appl. Catal. B: Environ. 49 (2004) 1-14.

[29] L. Wang, Z. Wang, D. Wang, X. Shi, H. Song, X. Gao, Solid State Sci. 31 (2014) 85-90.

[30] X. Guo, C. Chen, W. Song, X. Wang, W. Di, W. Qin, J. Mol. Catal. A: Chem. 387 (2014) 1-6.

[31] A. Tang, Y. Jia, S. Zhang, Q. Yu, X. Zhang, Catal. Commun. 50 (2014) 1-4.

[32] Y.C. Lin, H.S. Lee, J. Hazard. Mater. 179 (2010) 462-470.

[33] S. Wang, K.K. Meng, L. Zhao, Q. Jiang, J.S. Lian, Ceram. Inter. 40 (2014) 5107-5110.

[34] P. Hou, F.S. Cannon, C. Nieto-Delgado, N.R. Brown, X. Gu, Chem. Eng. J. 223 (2013) 309-317.

[35] L. Rizzo, S. Meric, D. Kassinos, M. Guida, F. Russo, V. Belgiorno, Water Res. 43 (2009) 979-988.

[36] Y. Liu, X. Chen, J. Li, C. Burda, Chemosphere 61 (2005) 11-18.

[37] D.C. Montgomery, Design and analysis of experiments, John Wiley & Sons, Newyork, 2001.

[38] R.H. Myres, D.C. Montgomery, Response Surface Methodology: Process and Product Optimization Using Designed Experiments, John Wiley and Sons, Newyork, 1995.

[39] A.L. Ahmad, S. Ismail, S. Bhatia, Environ. Sci. Technol. 39 (2005) 2828-2834.

[40] MSDS of Aeroxide P25. http://www.acros.be/DesktopModules/Acros_Search_Results/Acros_Search_Results.aspx?search_type=CatalogSearch&SearchString=38429.2014. Acros Organics.

[41] S. Sakthivel, H. Kisch, Angew. Chem. Int. Edit., 42 (2003) 4908-4911.

[42] M.V. Kulkarni, B.B. Kale, Sensor Actuat B: Chem. 187 (2013) 407-412.

[43] S. Debnath, N.R. Roy, U.C. Ghosh, Inter. J. Green Nanotechnol. 3 (2011) 271-280.

[44] E.K. Goharshadi, M. Hadadian, M. Karimi, H. Azizi-Toupkanloo, Mater. Sci. Semicond. Process. 16 (2013) 1109-1116.

[45] S. Song, L. Xu, Z. He, H. Ying, J. Chen, X. Xiao, B. Yan, J. Hazard. Mater. 152 (2008) 1301-1308.

[46] M.A. Rauf, M.A. Meetani, S. Hisaindee, Desalination 276 (2011) 13-27.

[47] I.H. Cho, K.D. Zho, Dyes Pigments 75 (2007) 533-543.

[48] N.B. Parilti, C.S.U. Demirel, M. Bekbolet, J. Photochem. Photobiol. A: Chem. 225 (2011) 26-35.

[49] K.P. Singh, S. Gupta, A.K. Singh, S. Sinha, J. Hazard. Mater. 186 (2011) 1462-1473.

Figure Captions

Figure 1: Schematic diagram of the annular reactor used for degradation of EY and NBB with PTO.

Figure 2: (A) Diffuse reflectance UV-visible spectra and (B) Tauc plot for Band gap energy of TO and PTO.

Figure 3: SEM image and EDS spectra of (A) PTO and (B) TO and (C) TEM image of PTO and inter lattice distance of PTO particles.

Figure 4: FTIR spectra of PTO and before and after degradation**.**

Figure 5: Effect of pH on (A) EY and (B) NBB degradation by PTO in presence of UV light.

Figure 6: Effect of dosage of PTO on (A) EY and (B) NBB degradation in presence of UV light.

Figure 7: Effect of initial concentration of (A) EY (B) NBB on degradation efficiency by PTO in presence of UV light**.**

Figure 8: Effect of intensity of UV light on degradation of (A) EY (B) NBB by PTO.

Figure 9: Response surface plots showing the effect of independent variables catalyst mass and pH on degradation of (A) EY and (B) NBB by PTO under UV light.

Figure 10: Response surface plots showing the effect of independent variables initial dye concentration and pH on degradation of (A) EY and (B) NBB by PTO under UV light.

Figure 11: Response surface plots showing the effect of independent variables initial dye concentration and catalyst mass on degradation of (A) EY and (B) NBB by PTO under UV light.

Figure 12: The LCMS spectra of the **(A)** EY before UV irradiation, **(B)** NBB before UV irradiation, **(C)** EY after 180 min UV irradiation and **(D)** NBB after 180 min irradiation in presence of PTO.

Scheme 1. Possible degradation products of EY after UV irradiation in presence of PTO, as determined by LC–MS spectrum given in **Figure 12 A and C**. Letters in parentheses are the species identified in **Figure 12 A and C**.

Scheme 2. Possible degradation products of NBB after UV irradiation in presence of PTO, as determined by LC–MS spectrum given in **Figure 12 B and D**. Letters in parentheses are the species identified in **Figure 12 B and D**.

Table

Table 1: Regression analysis and significance of the components in the quadratic model for EY and NBB degradation by PTO in presence of UV light

Variables		Symbol	Factor code	Level of factors		
				- 1	0	+ 1
Initial dye concentration (mg.L^{-1})		C_o	X_1	3.0	6.2	11
pH		pH	X_2	15	30	60
Adsorbent dosage (g.L^{-1})		m	X_3	0.25	0.50	1.0

Run	Coded levels			Observed degradation (%)		Predicted degradation (%)		Residual	
	X_1	X_2	X_3	EY	NBB	EY	NBB	EY	NBB
1	-1	-1	+1	99.85	99.74	96.76	98.20	-3.09	-1.54
2	-1	-1	-1	94.56	95.65	94.18	93.69	-0.38	-1.96
3	-1	0	0	98.91	99.66	100.7	99.62	1.84	-0.04
4	0	0	+1	98.93	99.11	97.36	95.18	-1.57	-3.93
5	+1	+1	+1	87.23	80.25	85.04	78.85	-2.19	-1.4
6	+1	-1	+1	95.68	98.56	98.59	99.05	2.91	0.49
7	0	0	0	98.91	96.93	98.29	94.77	-0.62	-2.16
8	+1	0	0	94.39	82.9	94.42	89.75	0.03	6.85
9	-1	+1	+1	85.32	87.54	89.26	91.73	3.94	4.19
10	0	0	0	98.91	96.93	98.29	94.77	-0.62	-2.16
11	0	0	0	98.91	96.93	98.29	94.77	-0.62	-2.16
12	0	0	0	98.91	96.93	98.29	94.77	-0.62	-2.16
13	-1	+1	-1	65.26	62.54	62.96	63.11	-2.3	0.57
14	0	0	-1	79.50	74.7	82.93	74.76	3.43	0.06
15	0	+1	0	81.33	80.06	78.55	78.94	-2.78	-1.12
16	+1	-1	-1	91.26	93.25	87.17	86.83	-4.09	-6.42
17	+1	+1	-1	46.56	41.26	49.89	42.52	3.33	1.26
18	0	0	0	98.91	96.93	98.29	94.77	-0.62	-2.16
19	0	-1	0	99.25	93.13	103.8	104.33	4.64	11.2
20	0	0	0	98.91	96.93	98.29	94.77	-0.62	-2.16

Table 2: Kinetic parameters for degradation of EY using PTO nanocomposite

Parameters	k_{LH} x 10^{-3} (min^{-1})		R^2		k_2 x 10^{-4} (mg.g^{-1}.min^{-1})		R^2		Half life (t$_{1/2}$) (min)	
	EY	NBB	EY	NBB	EY	NBB	EY	NBB	EY	NBB
Concentration (mg.L^{-1})										
15	56.43	85.85	0.9815	0.9836	78.52	131.1	0.9788	0.9864	10.46	6.48
30	27.11	29.18	0.9893	0.9624	19.35	22.53	0.9744	0.9929	23.45	20.96
60	23.54	16.03	0.9930	0.9599	8.63	6.76	0.9753	0.9873	27.01	33.00
Catalyst dosage (g.L^{-1})										
0.25	11.17	10.3	0.9928	0.9877	7.59	7.99	0.9462	0.9474	69.08	102.7
0.50	27.11	29.2	0.9903	0.9836	19.61	22.51	0.9726	0.9864	24.00	30.24
1.00	49.95	36.9	0.9923	0.9834	36.18	28.82	0.9568	0.9708	13.60	25.68
pH										
3.0	27.92	25.10	0.9864	0.9676	19.82	18.48	0.9683	0.9847	23.42	21.33
6.2	27.13	29.18	0.9893	0.9836	19.35	22.53	0.9744	0.9864	23.45	20.96
11.0	12.54	12.07	0.9970	0.9887	8.06	9.07	0.9426	0.9707	59.91	51.60
Light intensity										
15W	16.63	12.51	0.9926	0.9904	11.65	9.08	0.9664	0.9742	37.99	47.87
25W	27.16	23.49	0.9893	0.9886	19.32	16.82	0.9744	0.9784	23.45	26.17
Dark	4.16	4.52	0.9839	0.9813	2.53	2.83	0.9207	0.9124	288.1	278.2
25W w/o PTO	4.77	4.97	0.9900	0.9898	3.53	3.77	0.9598	0.9725	150.9	125.7

Table 3: Analysis of variance of the developed quadratic model for EY and NBB degradation by PTO in presence of UV light

Sources of variation	Sum of squares		Degree of freedom		Mean square		F value		Probability > F	
	EY	NBB	EY	NBB	EY	NBB	EY	NBB	EY	NBB
Model	3478.66	3974.88	9	9	386.52	441.65	32.00	15.84	<0.0001	<0.0001
C_o	78.11	241.46	1	1	78.11	241.46	6.46	8.65	0.0292	0.0147
pH	1240.32	1594.80	1	1	1240.32	1594.80	102.67	57.19	<0.0001	<0.0001
M	882.17	1033.94	1	1	882.17	1033.94	73.02	37.07	<0.0001	0.0001
C_o*pH	18.90	97.37	1	1	18.89	97.37	1.56	3.49	0.2395	0.0912
C_o*m	40.79	31.04	1	1	40.78	31.049	3.37	1.11	0.0960	0.3161
$pH*m$	291.11	300.79	1	1	291.11	300.79	24.09	10.71	0.0006	0.0082
C_o^2	0.32	0.016	1	1	0.3195	0.016	0.026	0.0006	0.8740	0.9813
pH^2	41.09	23.42	1	1	41.09	23.42	3.40	0.84	0.0949	0.3810
m^2	296.43	202.25	1	1	296.43	202.25	24.53	7.25	0.0006	0.0226
Lack of fit	120.80	278.84	5	5	24.16	55.77				
Pure error	0.000	0.00	5	5	0.000	0.00				
Residual	120.80	278.84	10	10	12.08	27.88				
Total	3599.46	4253.73	19	19						

Table 4: Coefficient of regression and standard errors

Source	Regression coefficient		Standard error	
	EY	NBB	EY	NBB
Constant	98.62	94.78	1.50	2.28
C_o	-2.80	-4.93	1.10	1.68
pH	-11.19	-12.69	1.10	1.69
m	9.43	10.21	1.10	1.68
C_o*pH	-1.51	-3.43	1.20	1.84
C_o*m	2.21	1.93	1.20	1.83
$pH*m$	5.93	6.03	1.21	1.83
C_o^2	0.39	0.08	2.39	3.64
pH^2	-4.16	-3.14	2.25	3.43
m^2	-11.87	-9.80	2.39	3.64
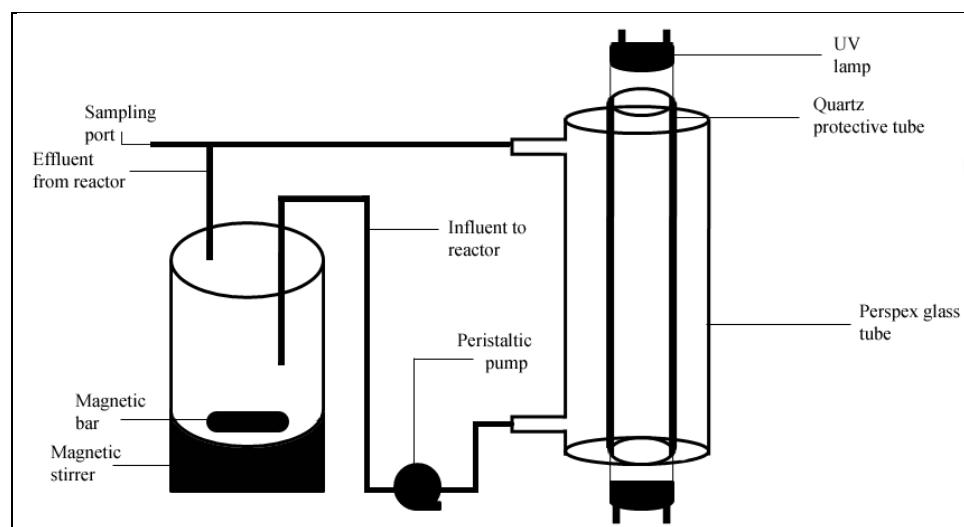
Figure
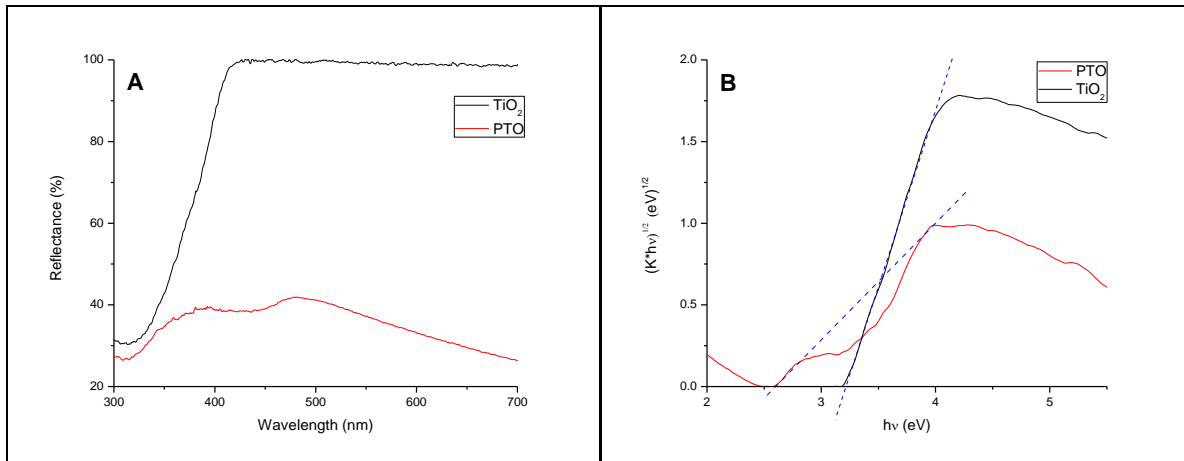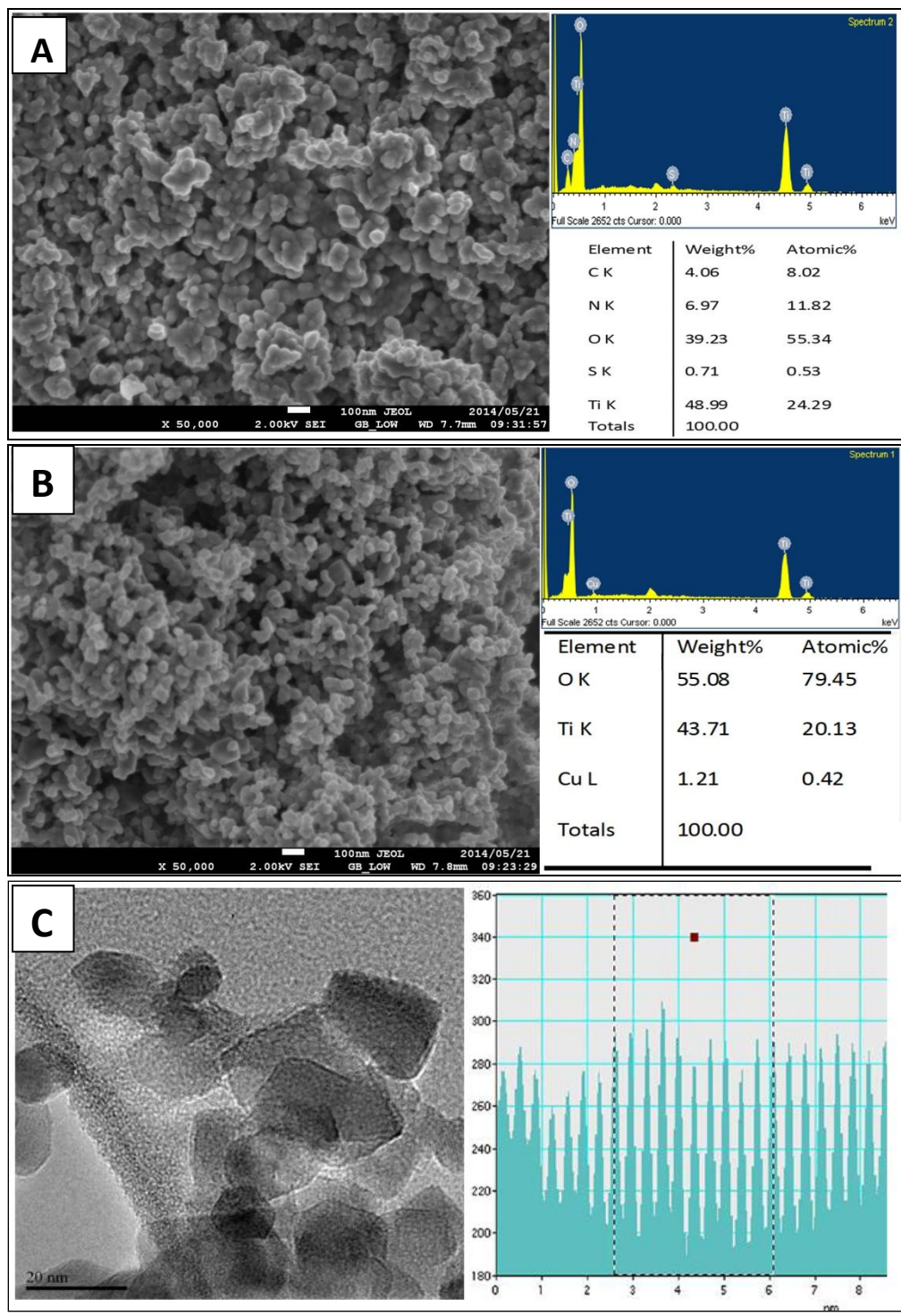
Figure 1

Figure 2

Figure 3
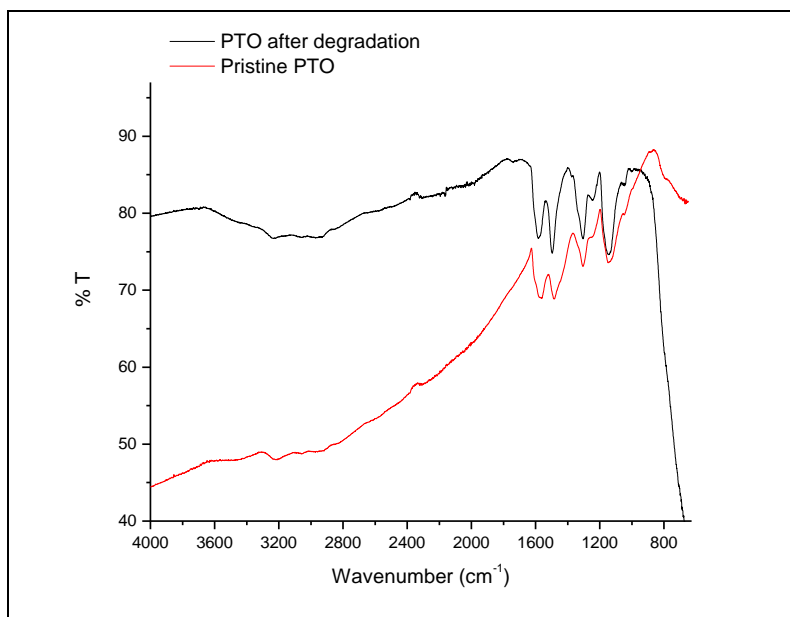
Figure 4
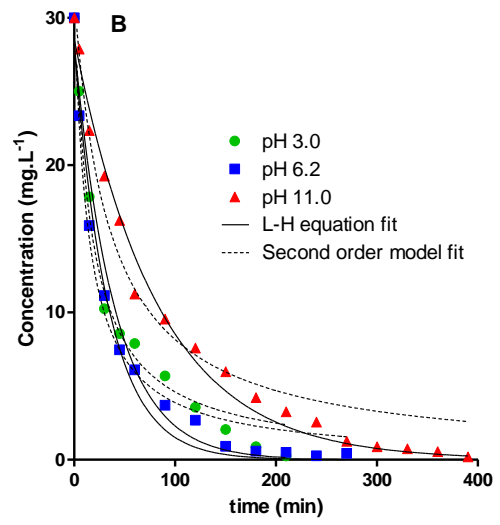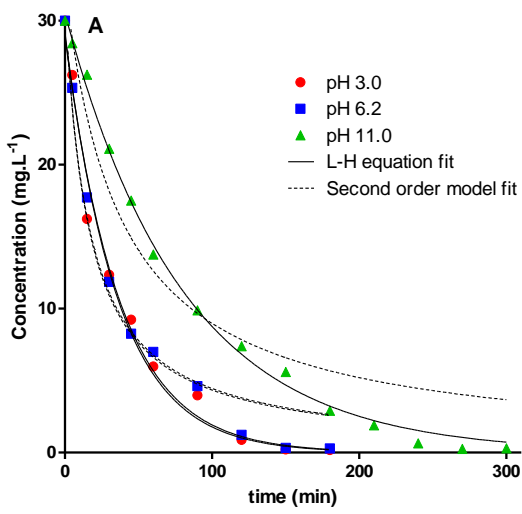
Figure 5
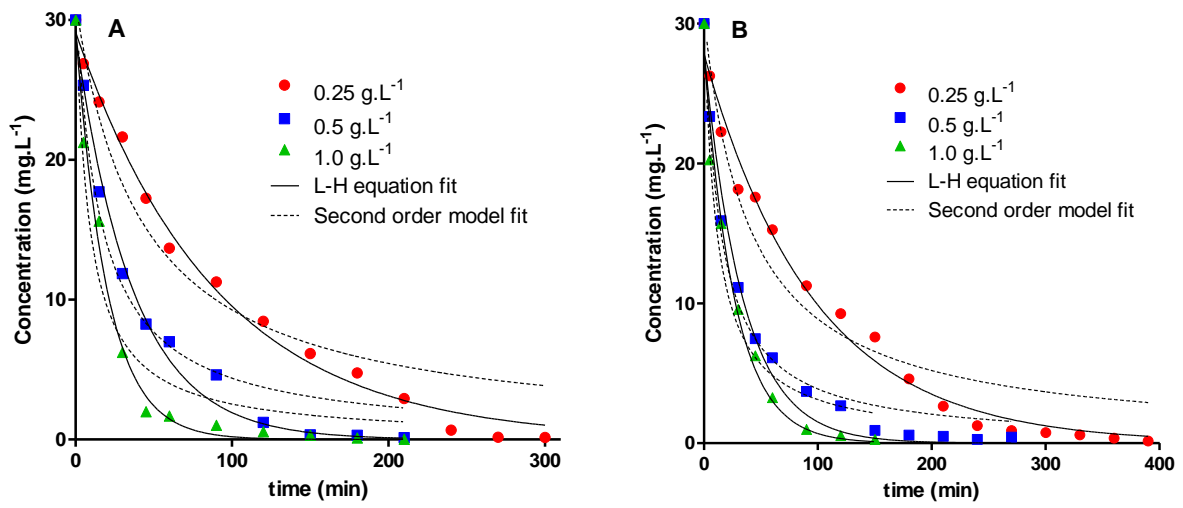
Figure 6
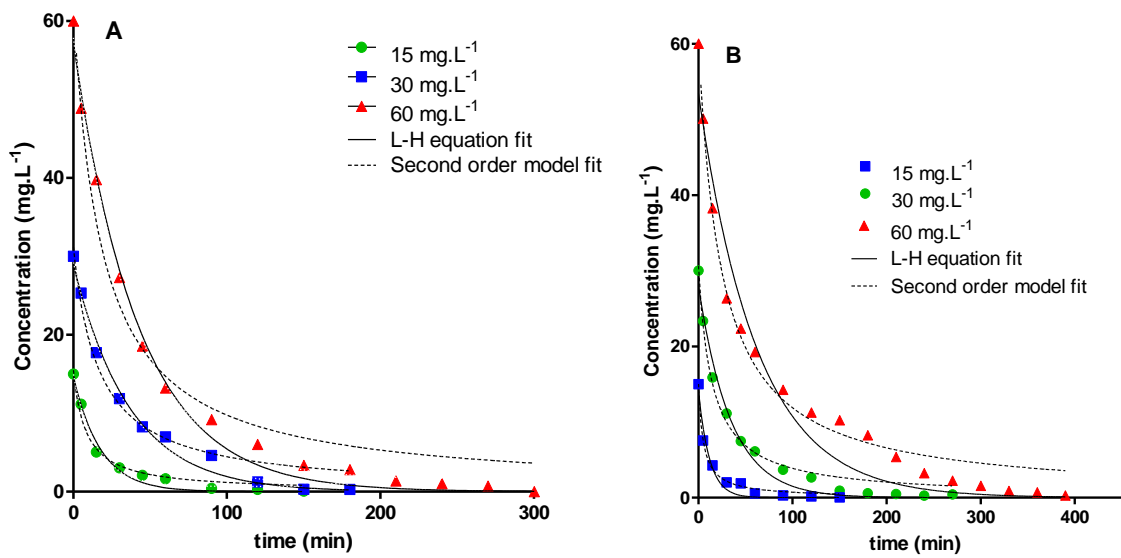
Figure 7
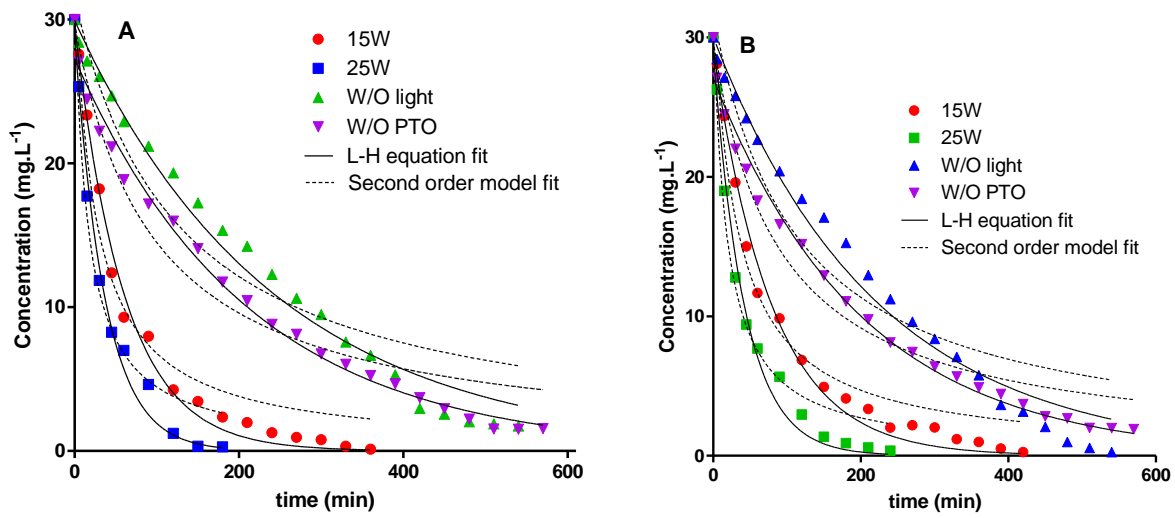
Figure 8
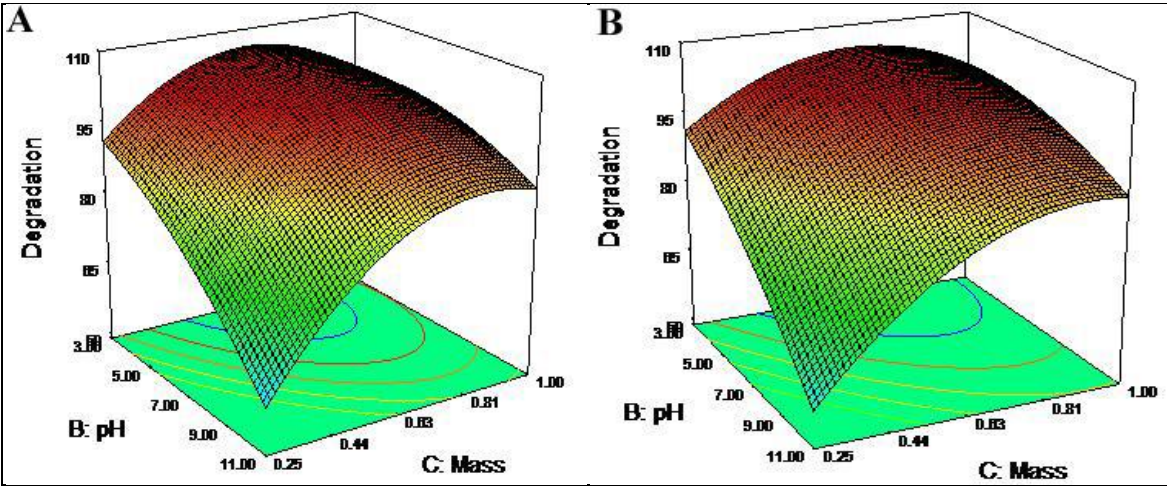
Figure 9
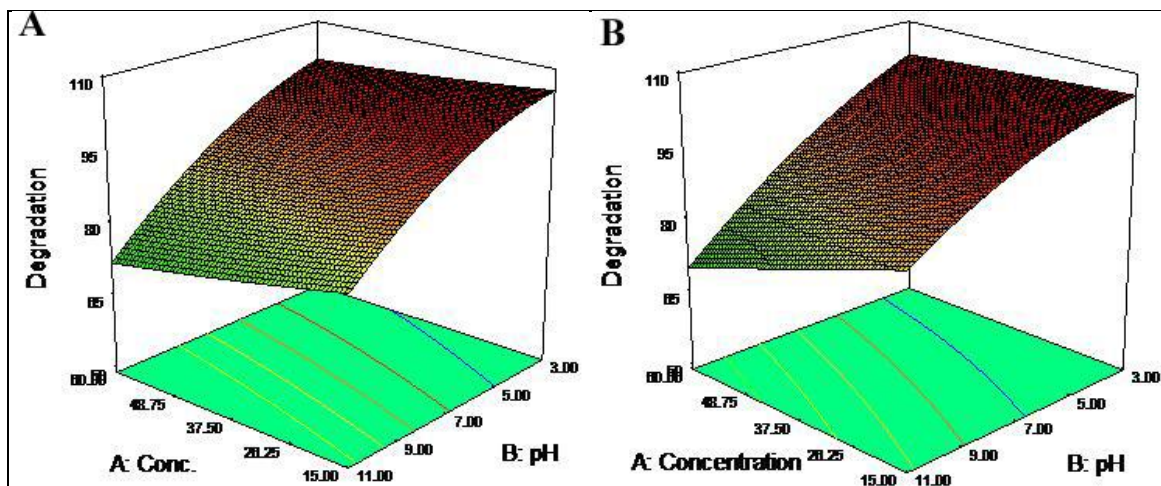
Figure 10
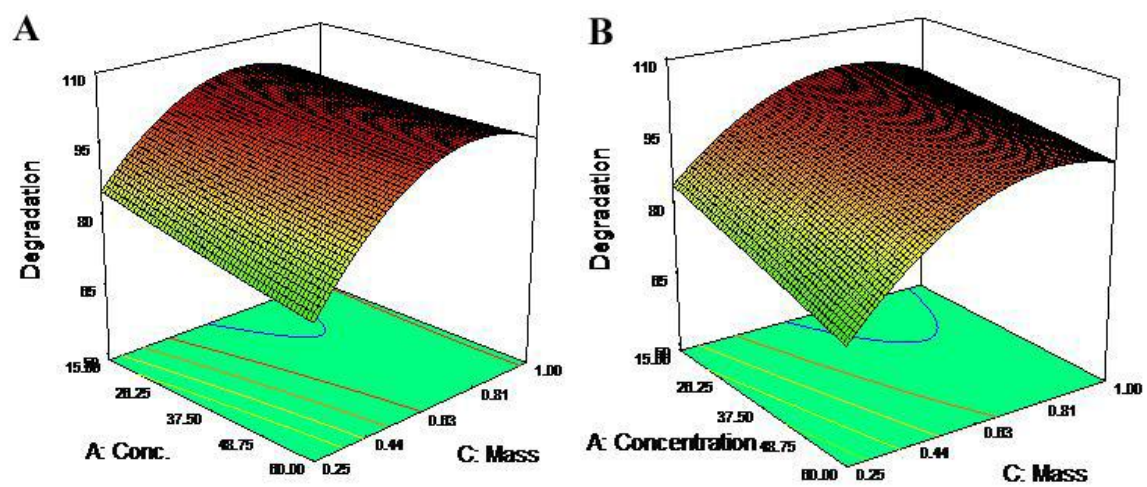
Figure 11
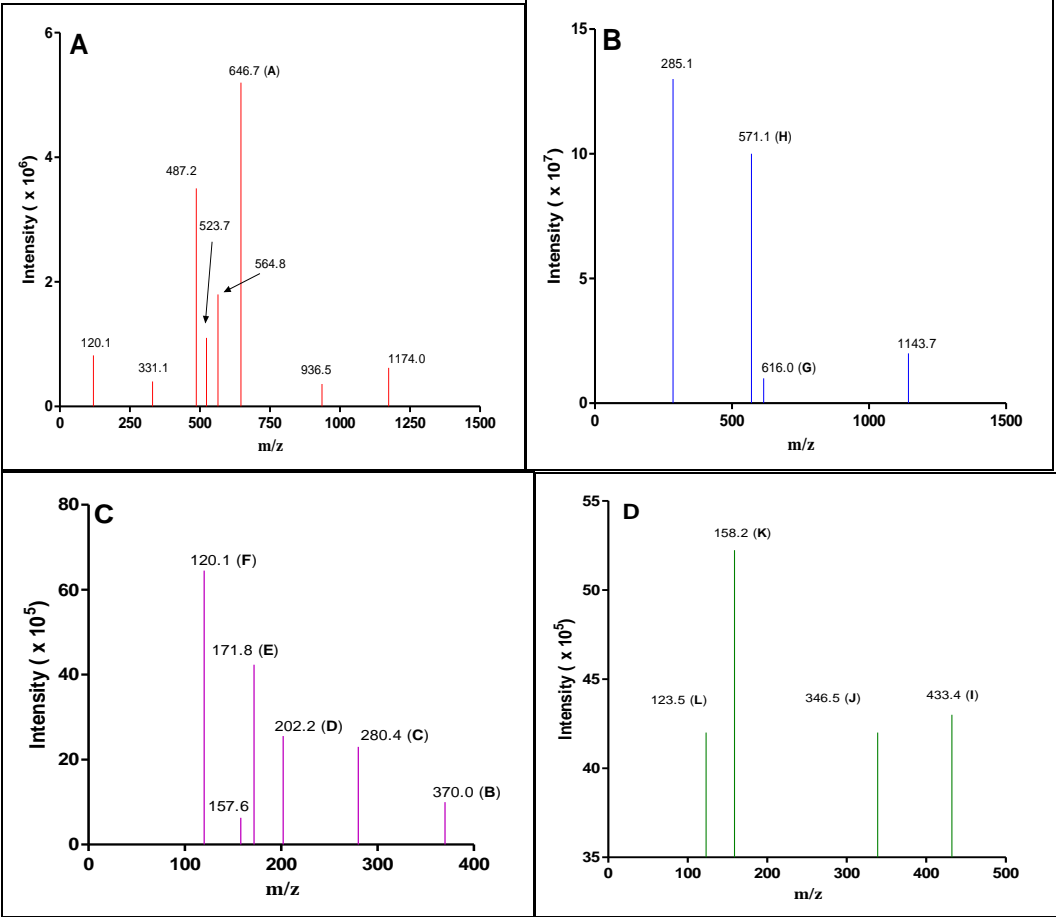
Figure 12
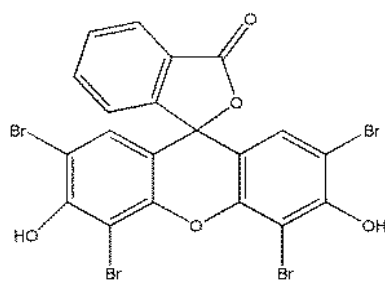
647.89 g/mol (A)
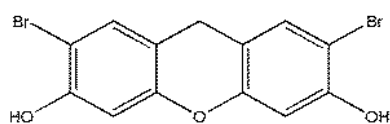
370.2 g/mol (B)
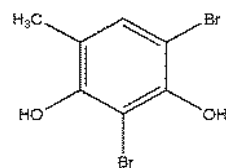
280.4 g/mol (C)
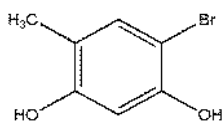
202.2 g/mol (D)
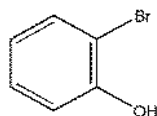
171.8 g/mol (E)

121.2 g/mol (F)

Scheme 1

616.49 g/mol (G)

570.5 g/mol (H)

433.2 g/mol (I)

346.5 g/mol (J)

158.7 g/mol (K)

123 g/mol (L)

Scheme 2

Aniline monomers

TiO_2

Polymerisation

hv_{UV}

$e^-_{Ti} \cdot h_{Ti}$

h^+_{Ti} = valance band hole

e^-_{Ti} = conduction band electron

$h^+_{Ti} + R_{Dye} \longrightarrow H \longrightarrow R^\bullet_{Dye} + H^+$

$h^+_{Ti} + H_2O \longrightarrow OH\bullet + H^+$

$h^+_{Ti} + O_2^{\bullet -} \longrightarrow O_2$

$e^-_{Ti} + O_2 \longrightarrow O_2^{\bullet -}$

$e^-_{Ti} + R^\bullet_{Dye} + H^+ \longrightarrow R_{Dye}$

A

Degradation

B: pH

C: Mass

B

Degradation

B: pH

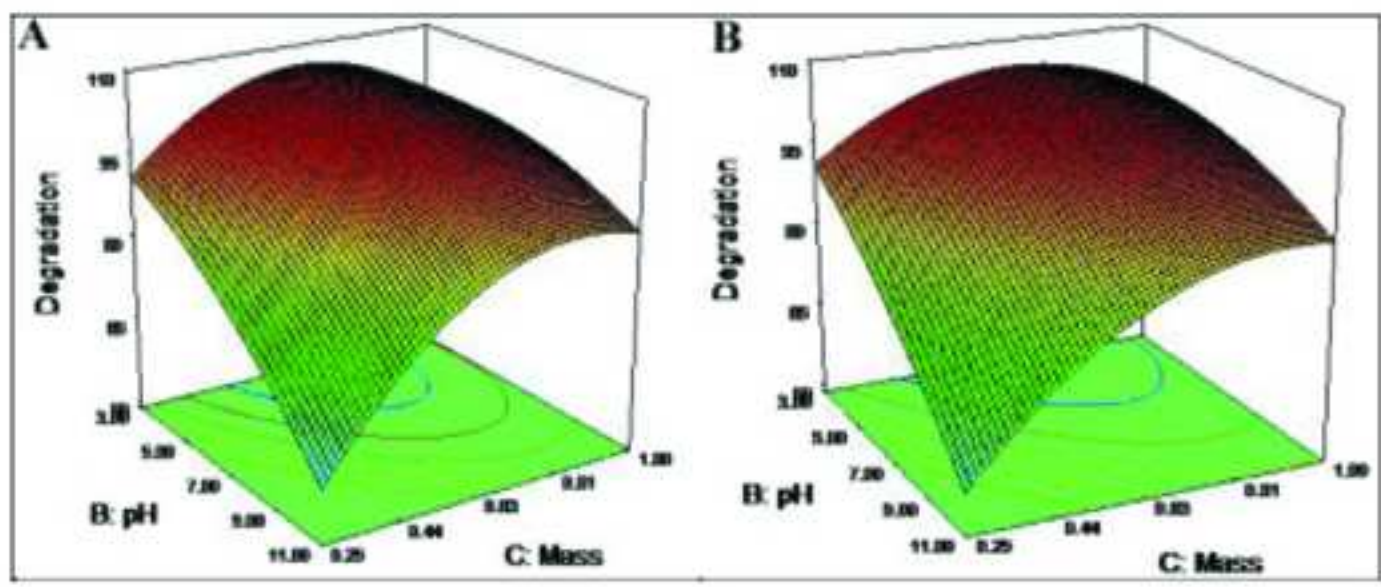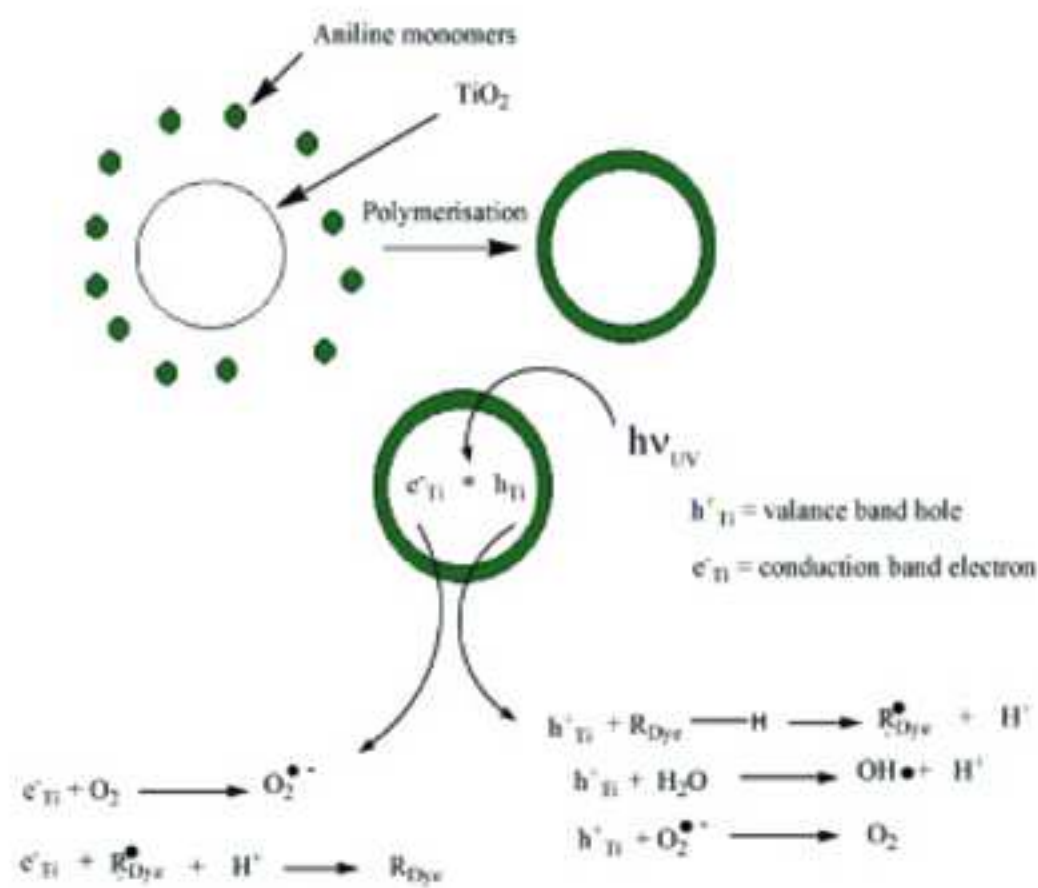C: Mass
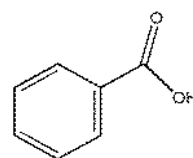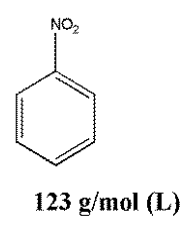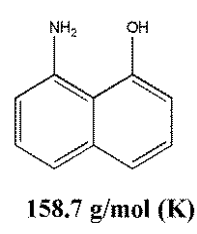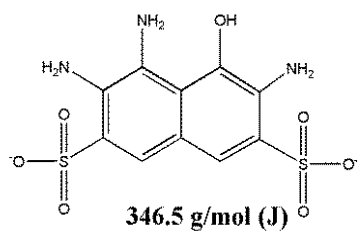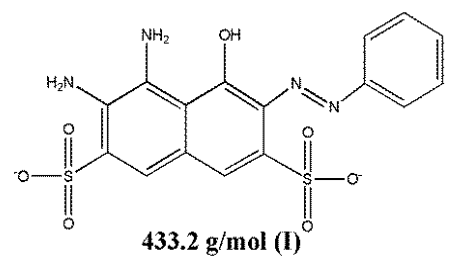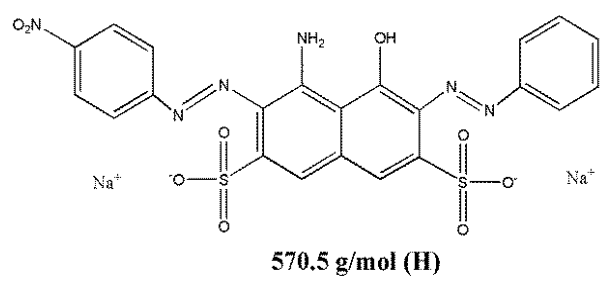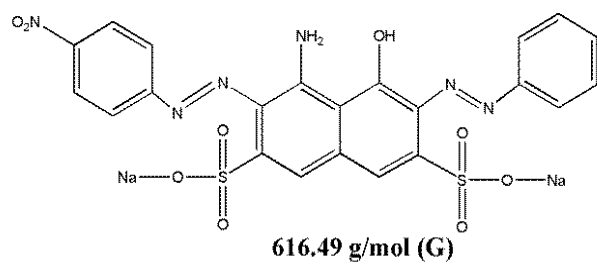
HIGHLIGHTS

- PTO nanocomposite was employed for degradation of Eosin Y and Naphthol Blue Black.

- Fast degradation achieved where 99% of 50 mgL^{-1} of dye was removed within 1 hour.

- Heterogeneous photocatalysis where degradation increased with increasing dosage.

- The degradation process was optimized by Response Surface Methodology.

- The degraded products were identified by LCMS and mechanism is proposed.

Supplementary Material